
YRiS **Yellow River Studies**

News Letter Vol.6

May 1, 2006

I.	Suspended sediment dispersion originated from the Yellow River in the Bohai Sea	2
II.	Analysis of long-term water balance of the Yellow River basin using the hydrological and water resources model -Impacts of the human activities-	9
III.	Study on Regional Income Inequality and Urbanization Mechanism in China.....	12
IV.	International activities related to YRiS	20

Suspended sediment dispersion originated from the Yellow River in the Bohai Sea

Guoqing CUI^{1*} and Tetsuo YANAGI²

¹Department of Earth Science and Technology, Graduate School of Engineering Science, Kyushu University, Fukuoka 816-8580, Japan

²Research Institute for Applied Mechanics, Kyushu University, Fukuoka 816-8580, Japan

1.Introduction

The Bohai Sea is connected to the Yellow Sea through the narrow Bohai Strait and contains three main bays, Liaodong Bay in the northeast, Bohai Bay in the west and Laizhou Bay in the south (Fig.1). The Yellow River is famous for its sediments load into the Bohai Sea. The average river discharge was $4.1 \times 10^9 \text{ m}^3$ per year and the sediment load was 0.54×10^8 tons per year in 2002 (MINISTRY OF WATER RESOURCE OF THE CHINA, 2002). The plume of suspended matter near the river mouth often visualizes the injection of Yellow River sediments into the Bohai Sea.

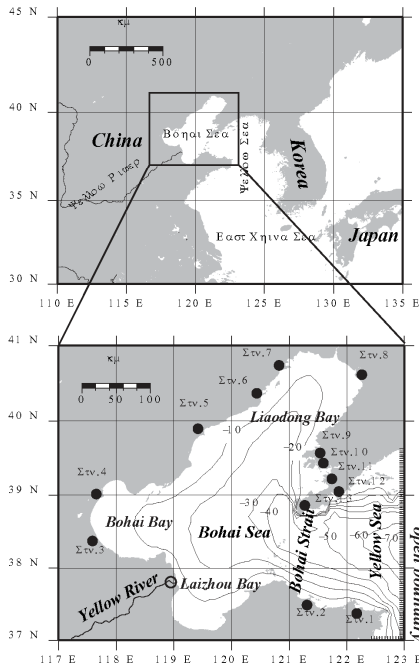


Fig.1 Bohai Sea is located in the northeast of China (upper panel). The modeled region is enlarged in the lower panel. Solid circles in the lower panel show the locations of 13 tide gauge stations. An open circle in the lower panel shows the grid location of the particle source (i.e. the Yellow River mouth).

There has been no study which explains the dispersion processes of the suspended sediment originated from the Yellow River in the Bohai Sea. In this study, we first develop a numerical model of tidal current and density-driven current in the Bohai Sea. Then, we investigate the transport processes of suspended sediment originated from the Yellow River using a three-dimensional suspended sediment transport model of the Bohai Sea. The objective of this study is to explain the spreading pattern of the suspended sediment dispersion originated from the Yellow River in the Bohai Sea.

2. Numerical model for the current

Short-term, seasonal and spring-neap tidal variations of the Yellow River plume in the Bohai Sea were investigated using NOAA AVHRR visible band images in 2002 (YANAGI and HINO, 2005). From this study, there was no distinct seasonal variation in the Yellow River plume spreading in the Bohai Sea. Thus, the wind-driven current is neglected in this numerical experiment, because the seasonal variation in the wind-driven current is very large in the Bohai Sea (JIANG and SUN, 2001). The tidal current, tide-induced residual current and density-driven current in the Bohai Sea are simulated by the Princeton Ocean Model (BLUMBERG and MELLOR, 1987).

The calculated tidal current ellipses at the surface for four major tidal constituents are shown in Fig.2.

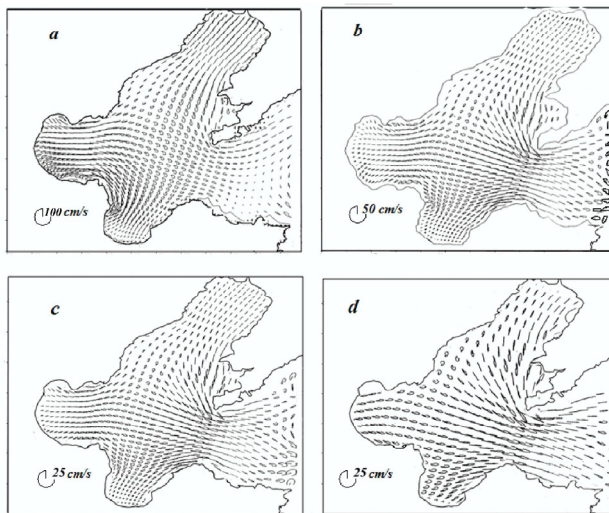


Fig.2 Distribution of M_2 (a), S_2 (b), K_1 (c) and O_1 (d) tidal current ellipses at the sea surface.

Based on these calculated tidal currents, we obtained the Eulerian and Lagrangian tide-induced residual currents. The maximum Eulerian tide-induced residual current by M_2 , S_2 , K_1 and O_1 tidal constituents, which was obtained by averaging the calculated results during 30 M_2 tidal cycles, is about 7 cm/s and it produces an anticlockwise flow along the coast of northern Bohai Bay and a clockwise flow along the coast of western Laizhou Bay at the surface as shown in Fig.3 (a). Above the bottom, the Eulerian tide-induced residual current is moderate or weak as opposed to the surface one as shown in Fig.3 (b). The Lagrangian tide-induced residual current is shown in Fig.3 (c) and (d). At the surface, the current speed is about 5 cm/s. However, in the central region of the Bohai Sea, the velocity is less than 1 cm/s. The Lagrangian tide-induced residual circulation forms a clockwise flow from Laizhou Bay to Bohai Bay along the coast. It is completely different from the Eulerian tide-induced residual current shown in Fig. 3 (a). Above the bottom, the Lagrangian tide-induced residual current is weak as opposed to the surface one.

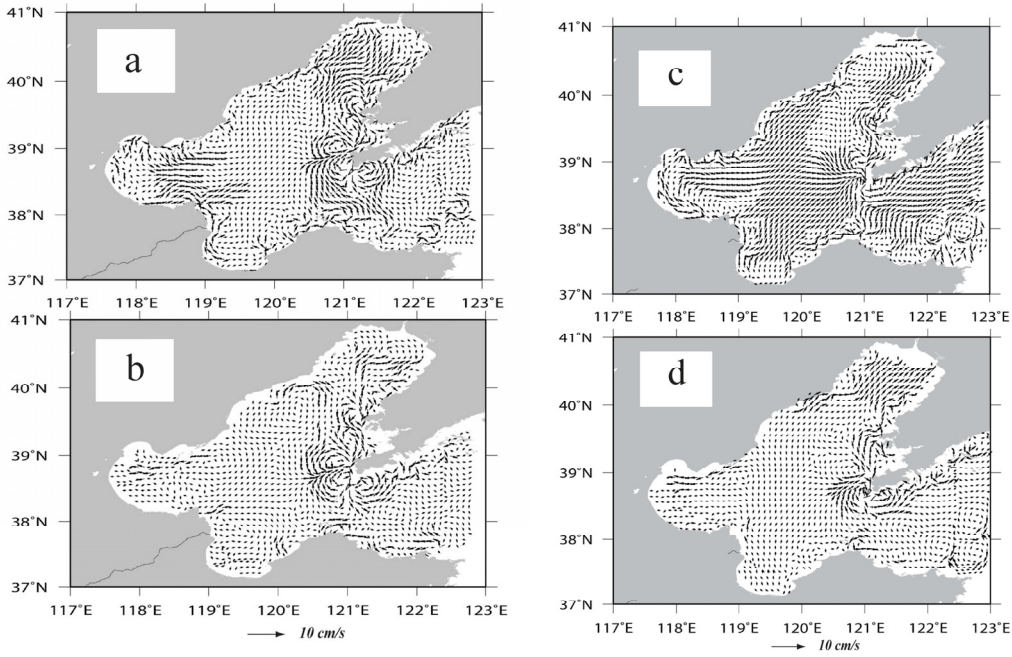


Fig.3 (a) Eulerian tide-induced residual current at the surface of the Bohai Sea, (b) Eulerian tide-induced residual current above the bottom, (c) Lagrangian tide-induced residual current at the surface of the Bohai Sea, and (d) Lagrangian tide-induced residual current above the bottom by M_2, S_2, K_1 and O_1 tidal constituents.

Because of the Coriolis effect, it is expected that the Yellow River fresh water spreads with the coast on the right hand side. The calculated result of the density-driven current shows that the southeasterly current exists at the surface around the Yellow River mouth (Fig.4 (a)). Above the bottom, the density-driven current is in the opposite direction to the surface one (Fig.4 (b)).

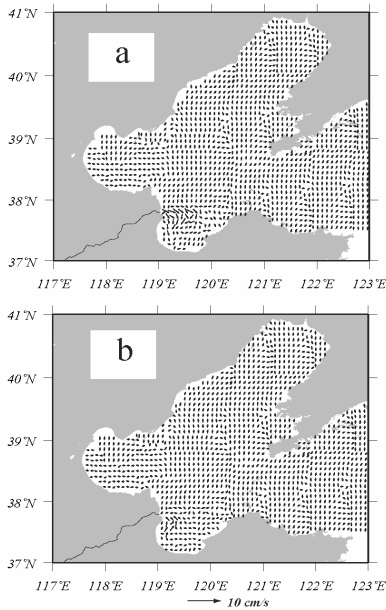


Fig.4 (a) Density-driven current at the surface of the Bohai Sea and (b) density-driven current above the bottom by the Yellow River discharge.

3 Suspended sediment dispersion originated from the Yellow River

In order to investigate the behavior of the suspended sediment dispersion originated from the Yellow River in the Bohai Sea, other experiments were conducted using the transport model with

the Euler-Lagrange method. The transport model is a 3D random walk model, which consists of two parts: 1) the movement of the suspended matter in the water body; 2) the deposition and re-suspension processes at the seabed. We can track the movement of material in a numerical model using the Euler-Lagrange method (YANAGI and INOUE, 1995) where the movement of a particle is tracked in the Lagrangian sense under the Eulerian current field.

From the sediment composition in the Yellow River at Lijin station (see Fig.1), silt (particles with the diameter of 4-64 μm) makes up about 75 % of suspended sediments (LI et al, 1998). In addition, the yearly averaged sediment diameter was 28 μm at Lijin station (MINISTRY OF WATER RESOURCE OF THE CHINA, 2002). Hence, we injected different sized particles (small, middle and large) with the same density of 2.5 g/cm^3 , which are shown in Table 1, from the Yellow River mouth.

Table. 1

	Small	Middle	Large
Diameter(μm)	4	30	50
Density(g/cm^3)	2.5	2.5	2.5

We conducted two experiments which correspond to spring tide and neap tide, because YANAGI and HINO (2005) showed that the spreading pattern in spring tide was different from that in neap tide as shown in Fig. 5.

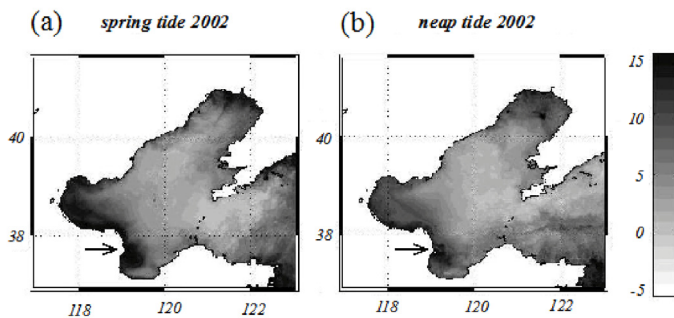


Fig.5 The Yellow river suspended sediments spreading from satellite images averaged in spring tide (a) and in neap tide (b) during 2002 (YANAGI and HINO, 2005).

In the first experiment, 200 particles were injected at spring tide and tracked until next spring tide for each particle size. In the second experiment, also 200 particles were injected at neap tide and tracked until next neap tide for each particle size as shown in Fig. 6.

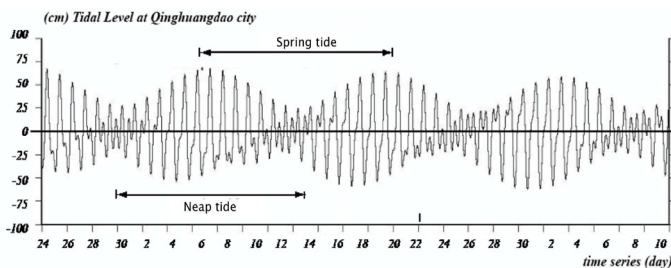


Fig.6 Calculated tidal level at Qinghuangdao City (Stn. 6 in Fig.1).

4. Calculated results

The calculated patterns of suspended sediments distribution injected from the Yellow River mouth in the Bohai Sea are shown in Fig.7 (a) and Fig.7 (b).

In the case of only considering the tidal current effect, the results show that most of small and middle sized particles from the Yellow River were transported mainly from Laizhou Bay to Bohai Bay with the coast on the left hand side as shown in Fig.7 (a). The spreading pattern well coincides with the Lagrangian tide-induced residual current in the surface layer, which is shown in Fig.3 (c). In the case of considering the tidal current and density-driven current effects, the results show that most of small and middle sized particles from the Yellow River were transported mainly from Laizhou Bay to Bohai Bay with the coast on the left hand side, and a part of small and middle sized particles from the river mouth were transported with the coast on the right hand side in Laizhou Bay near the river mouth as shown in Fig. 7 (b). This is due to that the Yellow River fresh water produces a clockwise density-driven current in the surface layer near the Yellow River mouth as shown in Fig. 4 (a). However, most of large sized particles were deposited within one day near the Yellow River mouth and they did not move again in both cases as shown in Fig.7.

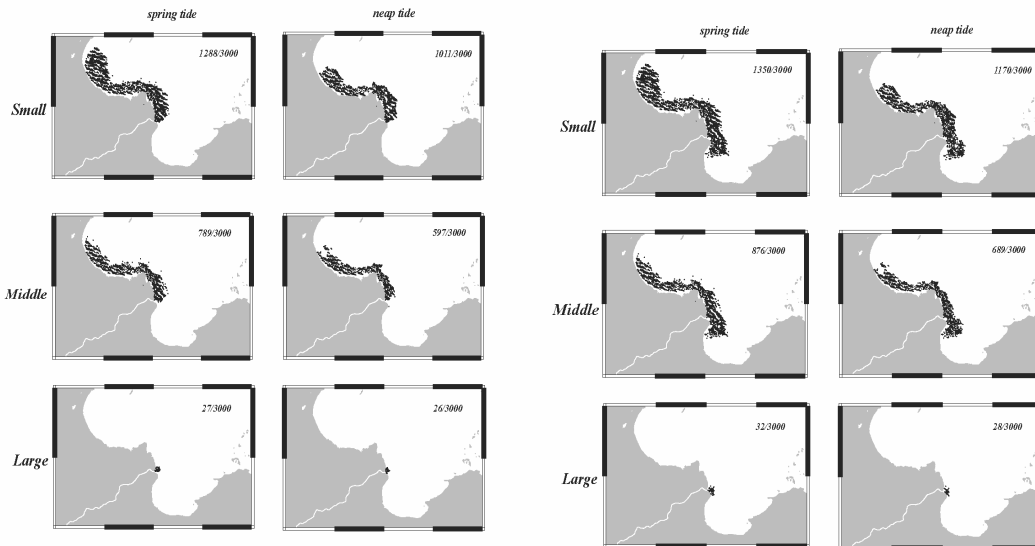


Fig.7 (a) Results of the calculation including only the tidal current effect. Upper number shows the total number of moving particles and lower number the total number of particles injected from the Yellow River mouth.

(b) those including the tidal current and density-driven current effects.

Furthermore, the spreading area during the spring tide is wider than that during the neap tide due to the re-suspension by the strong tidal current as shown in Fig. 7 (a) and (b). This is in agreement with the results from satellite images shown in Fig.5 (YANAGI and HINO, 2005).

5. Conclusion

The used transport model is a 3D random walk model, which consists of two parts: 1) the movement of the suspended matter in the water body and 2) the deposition and re-suspension processes at the seabed. The results from the numerical simulation by the transport model could explain the spreading pattern of the suspended particles observed from satellite.

The important findings in this study are: 1) the spreading area of the suspended particles during spring tide is wider than that during neap tide due to the re-suspension by the strong tidal

current, and 2) the spreading pattern of the suspended particles from the Yellow River in the Bohai Sea is mainly determined by the Lagrangian tide-induced residual current and the density-driven current.

References

- BLUMBERG, A.F. and G.L. MELLOR. 1987. A description of a three-dimensional coastal ocean circulation model, in three-dimensional coastal ocean models. *Coastal Estuarine Sci.*, 4, 1-208.
- JIANG, W. S. and W. X. SUN. 2001. 3D suspended particulate matter transportation model in the Bohai Sea II. Simulation results. *Oceannologia et Limnologia Sinica*, 32(1), 94-100.
- LI, G. X., H. L. WEI and HAN. 1998. Sedimentation in the Yellow River delta, part I: flow and suspended sediment structure in the upper distributary and the estuary. *Marine Geology*, 149, 93-111.
- MINISTRY OF WATER RESOURCES OF THE CHINA. 2002. *Report of river sediment in China*, 22pp, (in Chinese).
- YANAGI, T. and K. INOUE. 1995. A numerical experiment on the sedimentation processes in the Yellow and East China Seas. *Journal of Oceanography*, 51, 537-552.
- YANAGI, T. and T. HINO. 2005. Short-term, seasonal, and tidal variations in the Yellow River plume. *La mer*, 43, 1-7

Analysis of long-term water balance of the Yellow River basin using the hydrological and water resources model -Impacts of the human activities-

Yoshinobu Sato^{*}, Yoshihiro Fukushima^{*}, Xieyao Ma^{**}, Masayuki Matsuoka^{***},
Jianqing Xu^{**} and Hongxing Zheng^{****}

^{*}Research Institute for Humanity and Nature

^{**}Frontier Research Center for Global Change, Japan Agency for Marine-Earth Science and Technology

^{***}Faculty of Agriculture, Dept. of Forest Science, Kochi University

^{****}Institute of Geographical Sciences and Natural Resources Research, Chinese Academy of Sciences

Abstract

We attempt to develop a hydrological and water resources model and procedures to clarify the influence of human activities on the river runoff of the Yellow River basin. Although there are various human activities that affect the river runoff, we focused on the following three factors: (1) reservoir operation, (2) irrigation water intake from the river channels and (3) land use change during the period from 1960 to 2000.

1. Introduction

In order to analyze the hydrological processes of the large river basin such as the Yellow River, it is necessary to take into consideration not only natural factors but also artificial factors. In particular, the operation of reservoir and water intake for the irrigation is two major human activities, which may have profound impact on hydrological cycle. Moreover, the artificial land-use change is another factor as it changes the amount of water losses from land surface by the evapotranspiration. In this study, we analyzed long-term (1960-2000) water balances of the Yellow River basin using high resolution (0.1 degree) hydrological and water resources model considering not only natural factors (such as climate changes) but also above all artificial factors.

2. Study area and outline of the model

The Yellow River is the second-largest (also the longest) river basin in China. It originates from the Tibetan Plateau, wanders through the northern semiarid region, crosses the loess plateau, passes through the eastern (North China) plain, and finally discharges into the Bohai Sea. In general, the basin is divided into the following four sub-basins: (1) Source area (upstream of Tangnaihai gauge), (2) Upper reach (between Tangnaihai and Toudaoguai gauges), (3) Middle reach (between Toudaoguai and Huayuankou gauges) and (4) Lower reach (downstream of Huayuankou gauge). However, herein we separated the upper reach into two regions by Lanzhou gauge to detect the influences of reservoir operations and irrigation water intake respectively. For the middle reach, we focused on the water balance at Sanmenxia gauge in this issue.

The model used in this study is based on the SVAT-HYCY model developed by Ma and Fukushima (2002). The original model is composed of three components: one-dimensional SVAT model, runoff formation model, and river routine model (Ma et al., 2005). In this study, we modified the procedure of actual evapotranspiration estimation. The potential evaporation is calculated according to the approach defined by Xu et al. (2005). Actual evapotranspiration is then regarded as a function of potential evapotranspiration, LAI and soil moisture content, which was proposed by Kondo (1994). The land use type of the basin was divided into five types (Type1: Barren and Urban; Type2: Grass and Shrub; Type3: Forest; Type4: Irrigated and Type5: Water and

Snow) based on the dataset classified by Matsuoka et al., (2005).

3. Results and discussion

3.1. Tangnaihai

According to the remote sensing data, more than 90 % of the land surface is covered by the grass in the upstream of Tangnaihai and there are no large dams and irrigation areas. Therefore, the discharge pattern at Tangnaihai gauge is mainly influenced by the natural factors. Figure 1 shows the monthly discharge at Tangnaihai gauge from 1960 to 2000, where there is good agreement between observed discharge and simulated one.

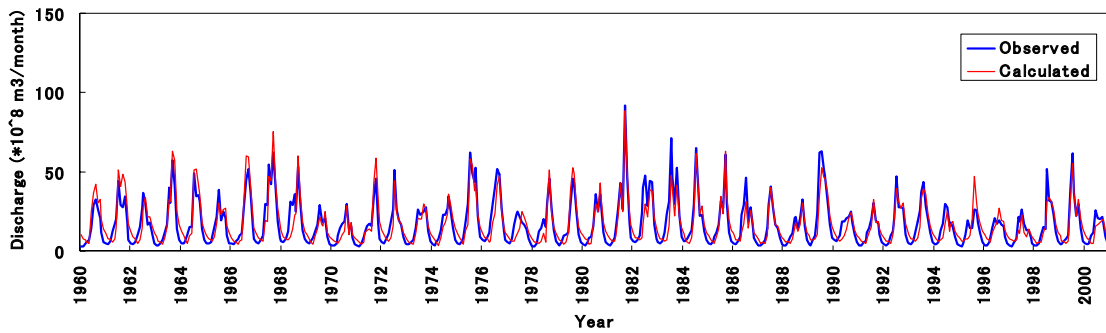


Figure 1 Monthly discharge at Tangnaihai gauge from 1960 to 2000.

3.2. Lanzhou

There are two large dams (Liujiaxia dam and Longyangxia dam) in the upstream of the Yellow River basin. Therefore, the observed discharge shows different seasonal change pattern to the natural discharge. According to the condition of the reservoir operation by the dams, we divided the period of analysis as follows: (1) from 1960 to 1968, no large dams existed in this period; (2) from 1969 to 1986, the river flow had been regulated lightly by the Liujiaxia dam; and (3) from 1987 to 2000, the river flow had been controlled strongly by the Longyangxia dam together with the Liujiaxia dam. Then, we extracted the reference seasonal discharge pattern (average monthly discharge pattern using the observed data except for the flood period) and applied it to the reservoir operation model developed by Sato et al. (2004). Figure 2 shows the performance of our model applied to the monthly discharge of Lanzhou gauge. This result suggests that our model can predict the various artificial controls by the dams (i.e. the peak flood mitigation or stable water supply during heavy water demand season) satisfactory.

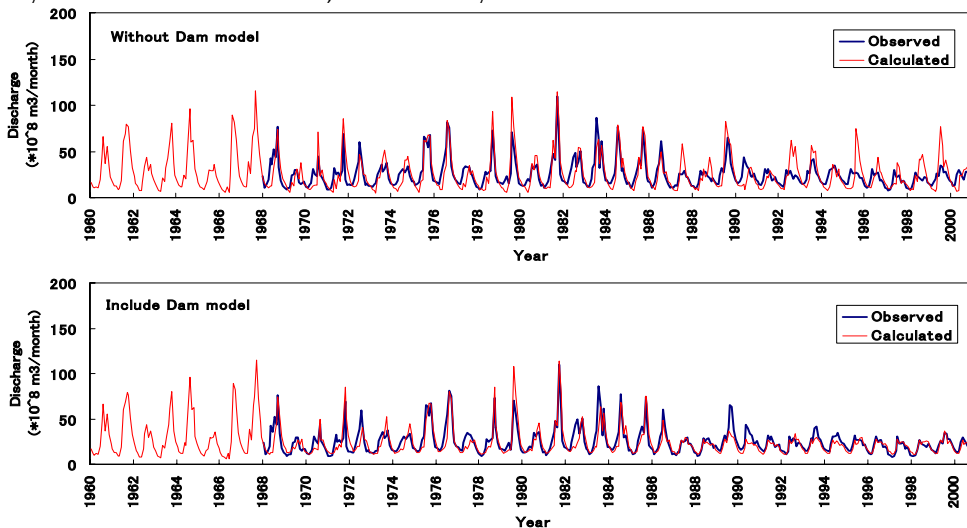


Figure 2 Comparison of monthly discharge at Lanzhou from 1960 to 2000 calculated by without dam model and include dam model.

3.3. Toudaoguai

Between Lanzhou and Toudaoguai, there are large irrigation areas include the Qingtonxia and Hetao irrigation districts, which consumes great amount of water from the river channel. According to the differences of observed discharge between Lanzhou and Toudaoguai (Lanz – Toud), it shows that almost 10 billions m^3 of river water lost in this area (Figure 3(d)). In this study, we analyzed the water balances of non irrigated area and irrigated area separately. In the irrigated area, the discharge from irrigated area during irrigation period was calculated by P (Gross Precipitation) – E_p (Potential Evaporation) and $P - E_a$ (Actual Evapotranspiration) for the non irrigation period. In our irrigation model, the negative discharge is corresponding to the water intake from river channel. The modeling results have shown that there is little discharge from non irrigated areas due to the dry climate condition, while the amount of actual evapotranspiration is almost the same to gross precipitation amount (Figure 3(a)). In the irrigated area, the amount of E_p exceeded more than three times of P . It suggests that in order to satisfy the water demand for the irrigation, it is necessary to intake more than 10 billion m^3 of water from the river channels continuously. Consequently, the total discharge from this area (Figure 3 (c)) became almost same amount of “Lanz - Toud” in Figure 3(d). We also found that the “Lanz - Toud” does not changed significantly during the past 40 years.

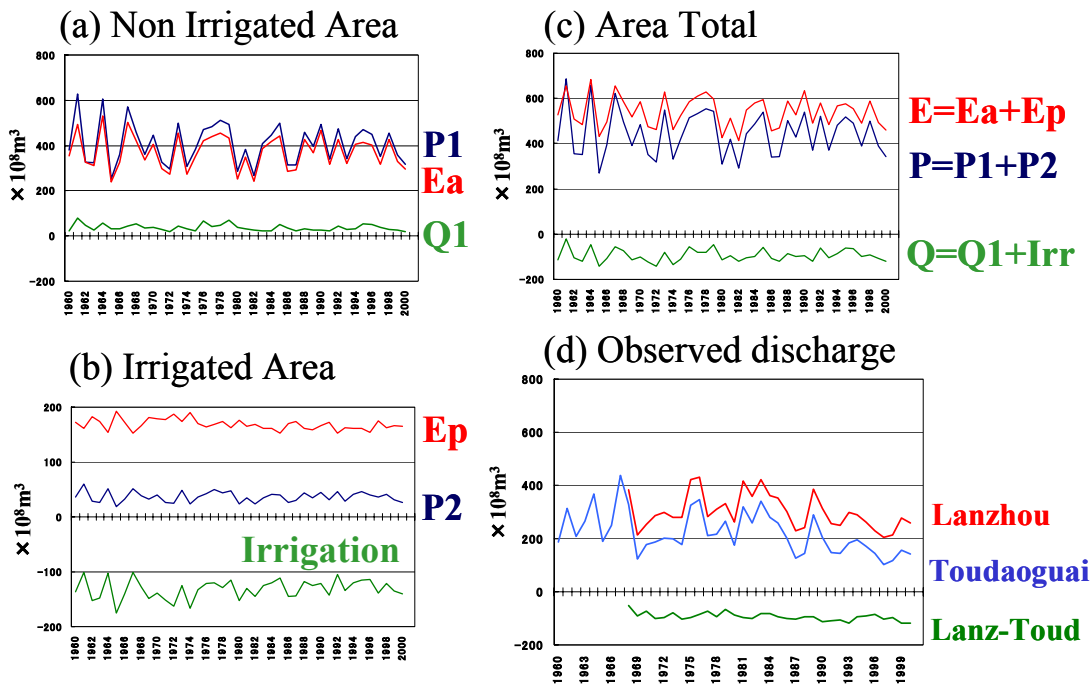


Figure 3 Water balance of the Irrigated area between Lanzhou and Toudaoguai.

3.4. Sanmenxia

In the middle reach, the calculated discharge from non irrigated area was also quite small (Figure 4 (a), which implies that most of the rain water was consumed within this middle reach.). It is correspondent to recent drying up of small tributaries in the middle reach. The estimated water loss by the irrigation was almost constant (Figure 4(b)). However, the estimated total discharge of Sanmenxia does not show a good agreement with observed values. In particular, it overestimates evapotranspiration in the 1960's to early 1970's, which has call for research efforts on long-term land use change.

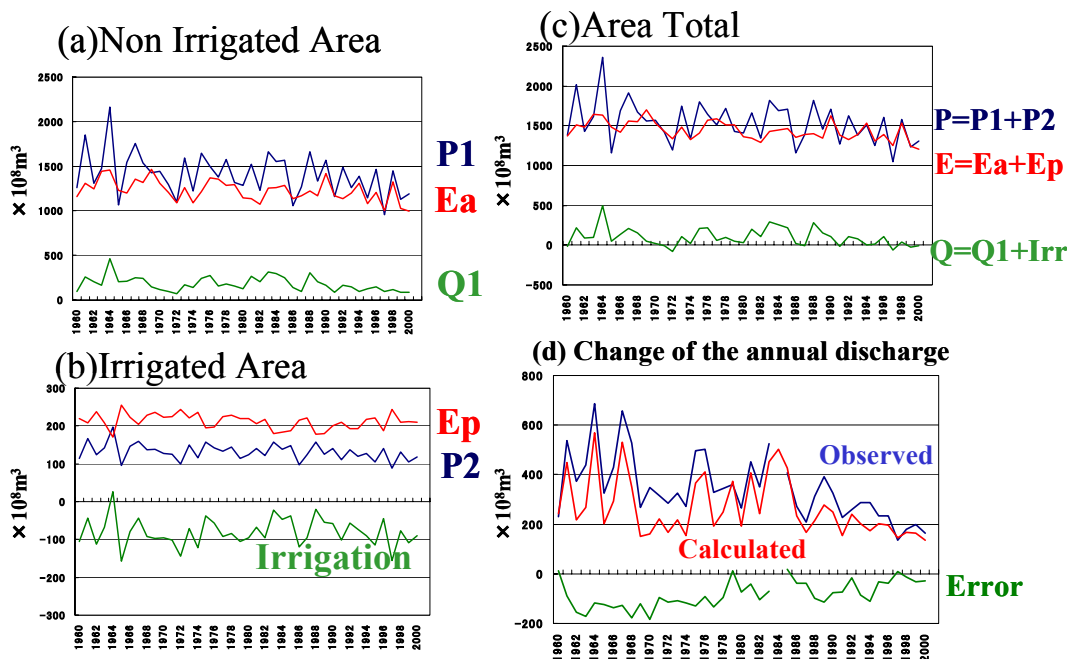


Figure 4 Water balance of the Middle reach of the Yellow River basin.

4. Conclusions

A modified version of hydrological and water resources model was developed and applied to the analysis of long-term water balances in the Yellow River basin. Modeling results have shown good agreement between observed discharge and simulated one not only in the source area (nearly natural status) but also upper reaches (under impacts of artificial factors such as dam operations and irrigation water intakes). However, it is still a challenge in modeling water cycle in the middle reach for its highly complexity. Further study is needed to improve our model to evaluate the influence of the long-term land use change.

References

- Kondo, J. 1994. Meteorology of the water environment, Asakura, Tokyo, 348 pp. (in Japanese)
- Ma, X., Fukushima, Y. 2002. Numerical model of river flow formation from to large scale river basin. In *Mathematical models of large watershed hydrology*, Singh VP, Frevert DK(eds). Water Resources Publications: Highlands Ranch, CO; 433-470.
- Ma, X., Fukushima, Y., Yasunari, T., Sato, Y., Matsuoka, M., Wu, X. and Zheng, H. 2005. Hydrological simulation in Tangnaihai and Lushi watersheds. *YRIS News Letter* 5: 1-5.
- Matsuoka, M., Hayasaka, Y., Fukushima, Y. and Honda, Y. 2005. Land cover classification over the Yellow River domain using satellite data. *YRIS News Letter* 4: 15-26.
- Sato, Y., Ma, X., Matsuoka, M, Hoshikawa, K., Fukushima, Y. 2004. Runoff Formation and Runoff Control System in Source Area of the Yellow River. Proceedings of 2nd International Workshop on Yellow River Studies, Nov.8-10, 2004 Kyoto, 95-98.
- Xu, J., Haginoya, S., Saito, K., Motoya, K. 2005. Surface heat balance and pan evaporation trends in Eastern Asia in the period 1971-2000. *Hydrological Processes* 19: 2161-2186.

Study on Regional Income Inequality and Urbanization Mechanism in China

Akio Onishi, Ji Han, Hidefumi Imura, Yoshihiro Fukushima

Abstract

China has been very successful at growing its economy since the start of economic reform in 1978. However, this rapid growth has also brought social issues in China. Currently, income inequality among regions is becoming one of the most notable issues. Within this socio-economic change, the release of resident registration system (“Hu-kou system”) has resulted in a great number of population migrations, and has caused the acceleration of urbanization in China. This urbanization must impact on environment, such as water use, energy consumption, land use change and pollution, etc..

This news letter measures the inequality among regions (Eastern region, Middle region, Western region) by using Gini coefficient and Theil index. Also, it estimates factors of inequality between Eastern region and Western region. Furthermore, mechanism of population migration is examined by using both nationwide time-series data and 2000 Census data.

1. Introduction

Since the start of economic reform in 1978, China has been experiencing a rapid socio-economic growth, accompanied by a dramatic changes, such as reform and opening-up, participation of WTO, expansion of regional gap, etc.. Within these changes, the release of resident registration system (“Hu-kou system”) has resulted in a great number of population migration, and has caused the acceleration of urbanization in China. The urbanization level grew from 18% to 36% from 1978 to 2000 in China. The total population migration from 1995 to 2000 amounted to over 100 million. The concentration of people in urban areas may contribute to economic growth by providing labors to urban development. On the other hand, this urbanization also has impacts on environment, such as water use, energy consumption, land use change and pollution, etc.. This report just focuses on the impact of human activity on water use, particularly on domestic water use. The regional income inequality and the mechanism of urbanization in China are analyzed in this report.

2. Regional Income inequality

Compared with 20 years ago or back to the 1980s, China's economy, measured by per capita GDP, is six times larger than before, and with an average annual growth rate at 9 %. The economy in provinces of eastern region grows much faster than those western inland areas (Figure 1). This spatial unbalanced economic growth has created a gap between regions in China. Generally, industrialization and urbanization are a pattern of

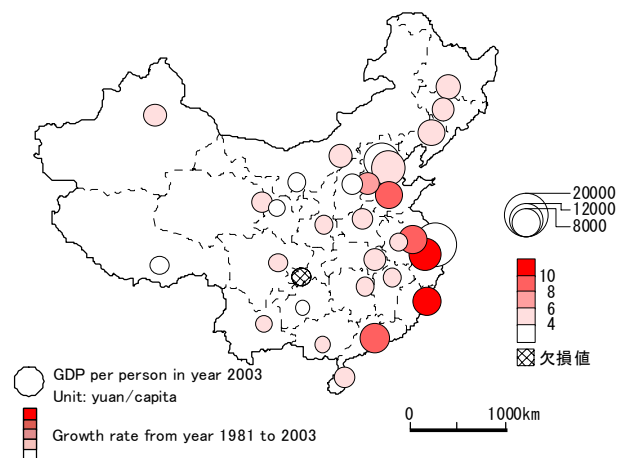


Figure1 GDP per person in 2003 and its growth rate from 1981-2003 in China

Notes: Eastern Region includes: Beijing, Tianjing, Hebei, Liaoning, Shanghai, Jiangsu, Zhejiang, Fujian, Shandong, Guangdong, Guangxi, Hainan. Middle Region includes: Shanxi, Inner Mongolia, Jilin, Heilongjiang, Anhui, Jiangxi, Henan, Hubei, Hunan, Shannxi. The rest belong to Western Region.

socio-economic development. Therefore, people migrate to cities to enjoy their development, which

including advanced education, high income, good medical treatment, and etc.. However, it is difficult to absorb all of these migrants because of limitation of jobs, accommodation, resources etc.. By this reason, China has been facing the issue of sustainable urbanization today.

2.1 Index of inequality

Gini coefficient and Theil index are classic methods to measure the inequality of income or economy between regions. This section shows results by adopting these methods to understand the fact of regional inequality in China. The Gini coefficient is shown as equation (1) (Gini, 1912). The value of the Gini coefficient lies between 0 and 1, where 0 indicates perfect equality (where everyone has the same income) and 1 indicates perfect inequality (where one person possesses entire income). There are many forms of formula for calculating the Gini coefficient, although the basic principle is the same. The Gini coefficient is calculated by equation (1) when per capita GDP in each province lies in lower values.

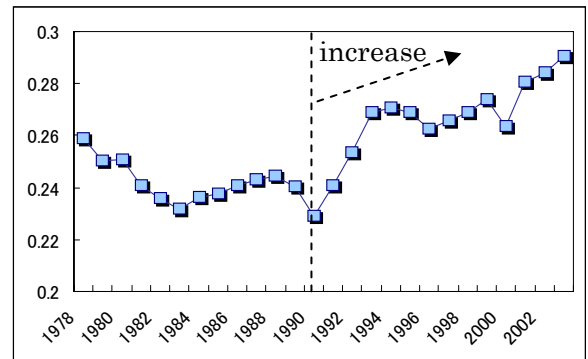
$$G_t = \frac{0.5 - \left[\sum_{i=1} \frac{p_{i,t}q_{i,t} - (p_{i,t}\gamma_{i,t})}{2} \right]}{0.5} \quad (1)$$

G : Gini coefficient, t : year (1978-2003), i : provinces, P : share of population, q : cumulated share of the GDP, γ : share of GDP

Result of the Gini coefficient was showed in Figure 2. It indicates that the inequality in China from 1978 to beginning of 1990s did not change dramatically. But after that, the disparity in China increased rapidly.

The Theil index, based on the concept of entropy, is defined by Theil (1967). It shares some characteristics with Gini coefficient, and ranges from 0 to 1. Theil index can show the contribution of intra-region inequality and inter-region inequality to total inequality.

Figure 2 Trend of income inequality in China (Gini coefficient)



$$T_p = \sum_i \sum_j \left(\frac{Y_{ij}}{Y} \right) \ln \left(\frac{Y_{ij}/Y}{P_{ij}/P} \right) \quad (2)$$

Y_{ij} : income of j provinces (autonomous districts) in region i , Y_i : $\sum Y_{ij}$, total of income in region i , Y : total of income in China

Income inequality in region i showed as T_{pi} can be defined by below equation;

$$T_{pi} = \sum_j \left(\frac{Y_{ij}}{Y_i} \right) \ln \left(\frac{Y_{ij}/Y_i}{P_{ij}/P_i} \right) \quad (3)$$

The Theil index is relatively easy for decomposition (as below) so that the contribution of

intra-region inequality and inter-region inequality to total inequality can be identified;

$$\begin{aligned}
 T_p &= \sum_i \left(\frac{Y_i}{Y} \right) T_{pi} + \sum_i \left(\frac{Y_i}{Y} \right) \ln \left(\frac{Y_i/Y}{P_i/P} \right) \\
 &= \sum_i \left(\frac{Y_i}{Y} \right) T_{pi} + T_{BR} \\
 &= T_{WR} + T_{BR}
 \end{aligned} \tag{4}$$

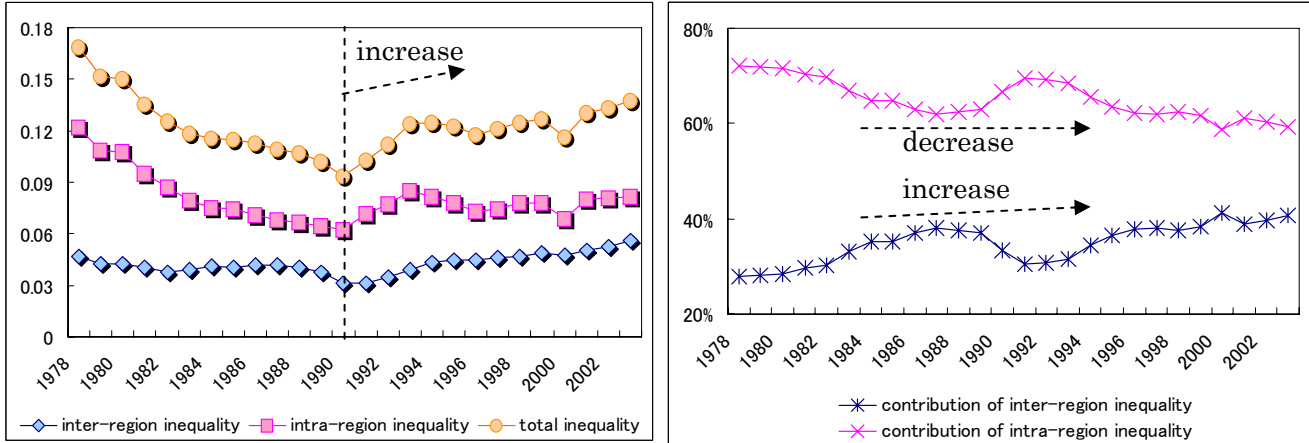


Figure 3 Trend of income inequality in China (Theil index)

Result of the Theil index was showed in Figure 3.

- The total inequality increases after 1990 in China same with the result of Gini coefficient.
- The inter-regional inequality has been increasing.
- On the other hand, the intra-regional inequality has been decreasing.

2.2 Factors of inequality

In this section, factors of inequality in China are analyzed by comparing Eastern region with Western region. In this analysis, data was from 1981 to 2000. And the regression model was showed as follows.

$$\ln(Y_{te} - Y_{tw}) = C + \alpha_1 \ln(E_{te} - E_{tw}) + \alpha_2 \ln(S_{te} - S_{tw}) + \alpha_3 \ln(I_{te} - I_{tw}) + \alpha_4 \ln(T_{te} - T_{tw}) + \mu_t \tag{5}$$

Y_{te} : per capita GDP in Eastern region in t year (fixed value of 2000)

Y_{tw} : per capita GDP in Western region in t year (fixed value of 2000)

E_{te} : ratio of employees of the second and third industries in Eastern region in t year

E_{tw} : ratio of employees of the second and third industries in Western coast region in t year

S_{te} : ratio of productions of the second and third industries in Eastern region in t year

S_{tw} : ratio of productions of the second and third industries in Western region in t year

I_{te} : per capita of Investment in Capital Construction in Eastern region in t year (fixed value of 2000)

I_{tw} : per capita of Investment in Capital Construction in Western region in t year (fixed value of 2000)

T_{te} : per capita of total export in Eastern region in t year (US dallor)

T_{tw} : per capita of total export in Western region in t year (US dallor)

μ_t : errors

- ① To identify the factors of inequality, four factors are selected as following; ① ratio of employees of the second and third industries, ② ratio of productions of the second and third industries, ③ per capita of Investment in Capital Construction, ④ per capita of total amount of

export. These factors suggest following meanings; ① inequality of job opportunity in the second and third industries, or inequality of speed of transformation to the second and third industries, ② inequality of speed of industrial transformation to the second and third industries, ③ inequality of investments which are to provide public services such as, water electricity, transport etc. by decision of governmental policy, ④ inequality of development of market economy.

The result was showed in Table 1.

Table 1 Factors of inequality by comparing Eastern region with Western region

Variables	Cochrane-Orcutt regression	
	coefficients	t statistic
<i>Constant</i>	3.91	7.40
a_1	0.41	2.72
a_2	-0.73	-3.42
a_3	0.16	3.05
a_4	0.51	6.16
<i>Adjusted R²</i>		0.94
<i>Durbin-Watson statistic</i>		1.87

This figure indicates below results;

- The factors to show East-West inequality are meaningful in statistics.
- The development of the market economy is a high contributor for inequality. The market of Eastern region has been more opened to foreign trade, compared with Western region.
- The job opportunity in the second and third industries is a significant factor for inequality.
- On the other hand, the gap of industrial transformation has been smaller between East-West. This result shows that industrial change in Western region has been smoothly ongoing. However, the shift of labors from agriculture to industry and service sections has not directly followed by industrial transformation. It is the one of the key point to solve the inequality whether the local industry can absorb employees in the second and third industries or not.
- The investments which are set as an index of governmental policy are a significant factor for inequality. After start the free trade, government has invested intensively to the Eastern region. This policy may have enhanced the inequality in China.

3. Characteristics of Population Migration and Urbanization in China

3.1 Scales and contribution of rural-to-urban migration to urbanization

The Figure 4 shows that urban population has been increasing and its rate become more than 30% of total population. On the other hand, rural population has been decreasing by less than 70% of total population (compare with 1952, it used to be 88%).

In order to see the contribution of migration to urbanization from 1983 to 2003, the urban population growth was decomposed into two parts: natural growth and net migration. As showed in table 2, the contribution of rural-to-urban migration to urban growth was 77% in 1983-1989, 67% in 1990-1995 and 86% in 1996-2003. It is obvious that the rural-to-urban migration turns out to be the dominant source of Chinese urban growth.

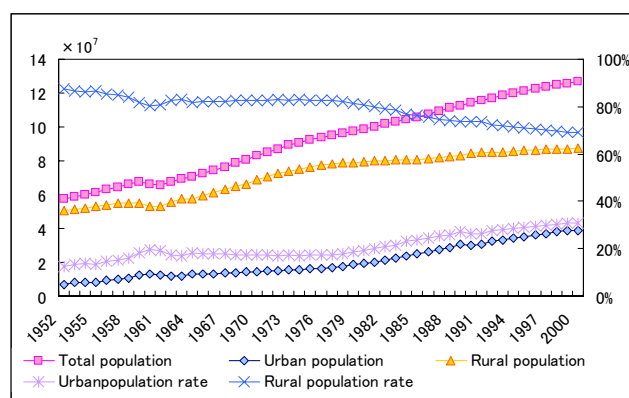


Figure 4 Population change in Urban and rural

Table 2 Contribution of rural-to-urban migration to urban population growth

Period	Annual growth of total urban pop. (million)	Annual natural growth of pop.		Annual net migration	
		Number (million)	Share (%)	Number (million)	Share (%)
1983-1989	11.52	2.69	23.3	8.83	76.7
1990-1995	9.39	3.08	32.8	6.31	67.2
1996-2003	21.50	2.96	13.8	18.54	86.2
1983-2003	14.71	2.90	19.7	11.81	80.3

Source: calculated from China Statistical Yearbook (NBS, 2000, 2004) and China Population Statistics

3.2 Spatial patterns of population migration

(A) Intra-provincial migration

According to the 5th National Census in 2000, within the total 128 million migrants, 73% were identified as the intra-provincial migrants, while 27% belonged to inter-provincial migration.

(B) Inter-provincial migration

For inter-provincial migration, as showed in Figure 5 and 6, the migration was primarily from the middle and western regions toward the eastern region. Guangdong, Shanghai, Zhejiang and Beijing became the concentrated centers. While Sichuan, Hunan, Anhui, Jiangxi were the largest senders of emigrants.

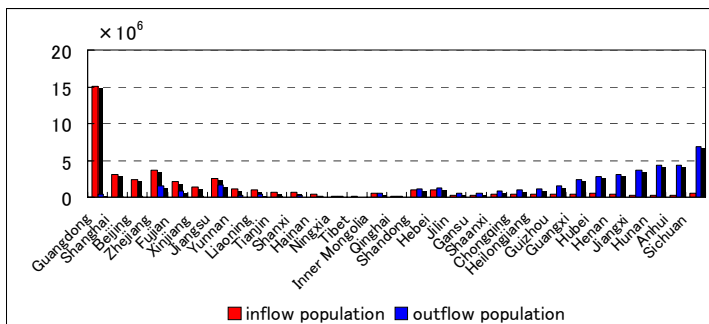


Figure 5 Provincial-level net in and out population migration (Unit: million)

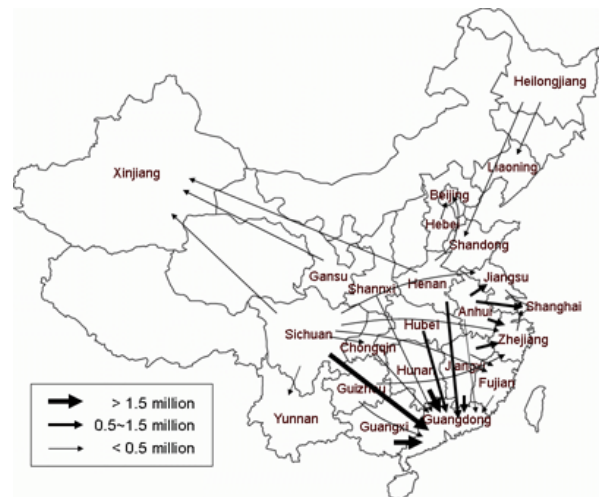


Figure 6 The 31 largest inter-provincial migration flow in 1995-2000 in China

(C) Migration between rural and urban areas

The total population migration can be divided into 4 categories in terms of the type of origin and destination. They are “rural-to-urban”, “rural-to-rural”, “urban-to-rural” and “urban-to-urban”. Among them, “rural-to-urban” was the largest one which shared 40.7% of the total migration. The second was “urban-to-urban” migration, which shared 37.2% of the total. The third was “rural-to-rural” migration, which shared 18.2% of the total. And “urban-to-rural” was the smallest, which only accounted for 3.9% of the total migration (Cai –Wang, 2003). In short, the primary population migration in China was the flow from rural areas to cities.

4. Analyses of the Mechanism of Population Migration

4.1 Analysis of time-series data

As discussed in the theories of development economy (Harris-Todaro, 1970), rural-to-urban migration should be a consequence of economic development. The following model of national

migration with time-series data in 1983-2003 was used to validate the theoretical assumption in China.

$$\ln M_t = C + a_1 \ln Y_t + a_2 \ln G_t + a_3 \ln U_t + a_4 \ln R_t + a_5 \ln T \quad (6)$$

where, subscript t denotes year; M is net rural-to-urban migration; Y is urban/rural per capita income ratio; G is per capita GDP; U is unemployment rate in cities; R is rural population per arable land; T is time dummy; C is constant.

In order to eliminate the effect of multicollinearity among variables, stepwise estimation method was adopted. Table 3 shows the results with and without stepwise estimation.

Table 3 Determinants of rural-to-urban migration in China 1983-2003

Variables	Full model		Model with stepwise estimation	
	coefficients	t statistic	coefficients	t statistic
<i>Constant</i>	-16.44	-1.43	-21.74***	-4.87
<i>Y</i>	-1.63	-1.59		
<i>G</i>	4.32***	4.39	4.72***	6.12
<i>U</i>	-1.42*	-1.93	-1.82**	-2.66
<i>R</i>	-1.32	-0.38		
<i>T</i>	-2.61**	-2.41	-3.38***	-5.24
Adjusted R^2	0.76		0.75	
F statistic	13.64***		21.18***	

*Level of significance: 10%; **Level of significance: 5%; ***Level of significance: 1%.

Economic level (measured by G) has a significant and positive effect on rural-to-urban migration.

- Urban unemployment has a significant and negative effect on rural-to-urban migration.
- The variables of urban/rural income ratio and rural population per arable land were supposed to have positive effect on rural-to-urban migration. But during the period 1983-2003 in China, the ranges of urban/rural income ratio (1.9-3.2) and rural population per arable land (8.0-9.1) changed little, causing a migration that did not respond significantly to these two variables.
- The significant and negative coefficient of T indicates a downward time trend in the level of migration. This may result from the administrative controls on the rural-to-urban migration.

4.2 Analysis of cross-section data

In order to further describe the patterns and mechanisms of population migration, an analytical model is established based on the cross-section data of 2000 Census.

$$\ln M_{ij} = C + \alpha_1 \ln(Y_j / Y_i) + \alpha_2 \ln(GDPR_j / GDPR_i) + \alpha_3 \ln(M_{ij} / \sum M_{ij}) + \alpha_4 \ln(DIS_{ij}) + \alpha_5 \ln(U_j / U_i) + \alpha_6 \ln(S_j / S_i) \quad (7)$$

where, M_{ij} is migration from province i to j ; Y is provincial per capita income; $GDPR$ is annual growth rate of provincial GDP; $M_{ij}/\sum M_{ij}$ is migration stock (measured by the proportion of emigrants from province i to each immigration province j . It implies the influence of old migrants on new migrants who plan to move); DIS_{ij} is distance between province i and j (measured by the shortest railway length between capital cities of two provinces); U is urban unemployment rate; S is share of the 2nd and 3rd industrial employment.

Table4 shows the results. And the major findings are as follows.

- In the eastern region, income gap is the most important determinant affecting migration.
- In the middle region, the share of second and third industrial employment is the most important

determinant affecting migration.

- In the western region, GDP growth rate is the most important determinant affecting migration.
- In whole China, income gap and migration stock have significant and positive effects on migration, while distance has a significant and negative effect on migration.
- In sum, the most important determinants of inter-provincial migration are income gap, migration stock and distance. Income gap and migration stock encourage migration while the distance discourages migration.

Table 4 Determinants of inter-provincial migration in China (with stepwise estimation)

Independent variables	Eastern Region		Middle Region		Western Region		Whole China	
	Coefficients	<i>t</i> statistic	Coefficients	<i>t</i> statistic	Coefficients	<i>t</i> statistic	Coefficients	<i>t</i> statistic
<i>Y</i>	0.84***	10.58			0.43**	2.39	0.62***	9.53
<i>GDP</i>					2.90***	7.17		
<i>Mstock</i>	0.77***	20.84	0.72***	21.52	0.66***	12.55	0.64***	23.89
<i>DIS</i>	-0.28***	-3.42	-0.42***	-5.00	-1.13***	-7.96	-0.83***	-13.17
<i>Unemploy</i>								
<i>S</i>			0.92***	6.59				
<i>Constant</i>	5.25***	9.98	6.69***	11.81	10.50***	11.63	8.74***	20.56
Adjusted <i>R</i> ²	0.77		0.82		0.61		0.65	
<i>F</i> statistic	385.06***		433.87***		107.40***		567.27***	

*Level of significance: 10%; **Level of significance: 5%; ***Level of significance: 1%.

Expected results for Next Steps

In this report, we showed the situation of regional income inequality and urbanization mechanism in China. The main findings are as follows;

- The inter-regional inequality has been increasing.
- This inequality has been created by inequality of job opportunity, miss leading of government policy, process of development of market economy.
- By this reason, after the release of resident registration system, people are inclining to migrate to more wealthy provinces, especially urban areas, in Eastern region.

Furthermore, we found some tasks to consider for next step;

- To more carefully identify inter-regional inequality, we should analyze what factors determine this inequality.
- To understand the impact of human activities such as migration and urbanization etc.on domestic water use.
- To more carefully identify other factors of migration.
- To expand socio-economic analysis to well understands the relationship between human activities and resources.

References

- Gini, C., 1912, Variabilità e mutabilità Reprinted in Pizetti E., Salvemini, T., eds., 1995, Memorie di metodologica (Libreria Eredi Virgilio Veschi, Rome).
- Theil, H., 1967, Economics and Information Theory (North-Holland, Amsterdam).
- Cai F., Wang D.W., Population migration as marketization: analysis of 5th census data. Population Science of China, 5, 11-19, 2003. (in Chinese)
- Harris J.R, Todaro M.P, Migration, unemployment and development: A two-sector analysis. American Economic Review, 60, 126-142, 1970.

International activities related to YRiS

(1) **Hydrological Sciences for Managing Water Resources in the Asian Developing World**, June 8-10, 2006, Guangdong International Hotel, Guangzhou, China
<http://cwre.zsu.edu.cn/mwra/index.htm>

(2) **Global Water System Project – 2nd Asian Meeting**, June 8-10, 2006, Guangdong International Hotel, Guangzhou, China

Yoshihiro Fukushima, Project Leader

Makoto Taniguchi, Secretary General

Research Institute of Humanity and Nature (RIHN),

Inter-University Research Institute

Ministry of Education, Culture, Sports, Sciences, and Technology, Japan (MEXT)

457-4 Motoyama Kamigamo, Kita-ku, Kyoto 603-8047, Japan

Tel: +81-75-707-2230, Fax: +81-75-707-2506

E-mail: YRiS@chikyu.ac.jp, URL: http://www.chikyu.ac.jp/index_e.html
